JOC*Article*

Negative Kinetic Temperature Effect on the Hydride Transfer from NADH Analogue BNAH to the Radical Cation of *N*-Benzylphenothiazine in Acetonitrile

Xiao-Qing Zhu,* Jian-Yu Zhang, and Jin-Pei Cheng*

Department of Chemistry, The State Key Laboratory of Elemento-Organic Chemistry, Nankai University, Tianjin 300071, China

xqzhu@nankai.edu.cn

Received June 5, 2006

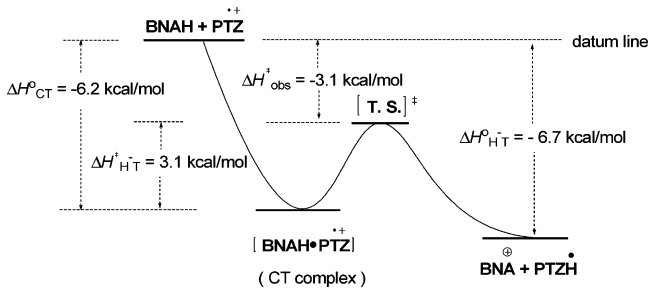

The reaction rates of 1-(*p*-substituted benzyl)-1,4-dihydronicotinamide (G-BNAH) with *N*-benzylphenothiazine radical cation ($PTZ^{\bullet+}$) in acetonitrile were determined. The results show that the reaction rates (k_{obs}) decreased from 2.80×10^7 to 2.16×10^7 M^{-1} s^{-1} for G = H as the reaction temperature increased from 298 to 318 K. The activation enthalpies of the reactions were estimated according to Eyring equation to give negative values (−3.4 to −2.9 kcal/mol). Investigation of the reaction intermediate shows that the charge-transfer complex (CT-complex) between G-BNAH and $PTZ^{\bullet+}$ was formed in front of the hydride transfer from G-BNAH to $PTZ^{\bullet+}$. The formation enthalpy of the CT-complex was estimated by using the Benesi−Hildebrand equation to give the values from −6.4 to −6.0 kcal/mol when the substituent G in G-BNAH changes from CH_3O to Br. Detailed thermodynamic analyses on each elementary step in the possible reaction pathways suggest that the hydride transfer from G-BNAH to $PTZ^{\bullet+}$ occurs by a concerted hydride transfer via a CT-complex. The effective charge distribution on the pyridine ring in G-BNAH at the various stages—the reactant G-BNAH, the charge-transfer complex, the transition-state, and the product $G\text{-}BNA^+$—was estimated by using the method of Hammett-type linear free energy analysis, and the results show that the pyridine ring carries relative effective positive charges of 0.35 in the CT-complex and 0.45 in the transition state, respectively, which indicates that the concerted hydride transfer from G-BNAH to $PTZ^{\bullet+}$ was practically performed by the initial charge (−0.35) transfer from G-BNAH to $PTZ^{\bullet+}$ and then followed by the transfer of hydrogen atom with partial negative charge (−0.65). It is evident that the present work would be helpful in understanding the nature of the negative temperature effect, especially on the reaction of NADH coenzyme with the drug phenothiazine in vivo.

Introduction

Hydride transfer is one of the fundamental chemical and biological reactions. The study of the hydride transfer from the nicotinamide−adenine dinucleotide coenzyme (NADH) and its analogues to the surrounding substrates[1] has been a subject of great interest and is increasingly drawing the attention of researchers due to the biological importance of NADH in living bodies.[2−10] Generally, the rate of hydride transfer would increase as the reaction temperature rises since an activation energy barrier should be overcome in the reaction.[11] But there is a case

(1) (a) Walsh, C. *Enzymatic Reaction Mechanism*; W. H. Freeman: San Fracisco, CA, 1979; Chapter 10. (b) Stryer, L. *Biochemistry*, 3rd ed.; W. H. Freeman: New York, 1988; Chapter 17. (c) Westheimer, F. H. In *Pyridine Nucleotide Coenzyme*; Dolphin, D., Poulson, R., Avramovic, O., Eds.; Wiley-Interscience: New York, 1988; Part A, p 253.

(2) (a) Murakami, Y.; Kikuchi, J.-I.; Hisaeda, Y.; Hayashida, O. *Chem. Rev.* **1996**, *96*, 721. (b) Stout, D. M.; Meyers, A. I. *Chem. Rev.* **1982**, *82*, 223. (c) Eisner, U.; Kuthan, J. *Chem. Rev.* **1972**, *72*, 1.

10.1021/jo061145c CCC: $33.50
Published on Web 08/10/2006

that the reaction rate could decrease as the reaction temperature rises, i.e., the lower the temperature, the faster the reaction rate.[12−28] This phenomena used to go by the name of negative kinetic temperature effect and was interpreted as follows: a reaction intermediate, the energy of which is lower than the reactant pair, lies in the course of reaction. Further, the energy difference between the reactant pair and the reaction intermediate is larger than the corresponding energy difference between the intermediate and the transition state of the reaction. Kiselev and Miller first reported the negative temperature dependence of rates for the Diels−Alder reaction of tetracyanoethylene with 9,10-dimethylanthracene via the reaction intermediate of the charge-transfer complex (CT-complex).[12] Later, Fukuzumi and co-worker observed the CT-complexes formed in the hydride transfer from the Michler's hydride to the quinone with the negative temperature dependence of rates.[27] Now, an interesting question, whether the negative temperature effect exists also in the hydride transfer from the nicotinamide−adenine dinucleotide coenzyme NADH in vivo, is worthy of attention. This question, in fact, has received our attention for a long time, since the solution of this question evidently is very important to understanding the practical kinetics of the hydride transfer from NADH in vivo.

By examining the past publications, it is found that except for the paper where Fukuzumi used 9,10-dihydroacridine as the NADH model and found the negative kinetic temperature effect on the reaction of 10-methyl-9,10-dihydroacridine with quinone,[28] no paper has reported the negative kinetic temperature effect on the hydride transfer from NADH or its analogues until now. Since 10-methyl-9,10-dihydroacridine is quite different from NADH in structure, it is evident that the observation of the negative kinetic temperature effect on the hydride transfer from 10-methyl-9,10-dihydroacridine to the quinone is not an efficient indicator that NADH could also have the same property of negative kinetic temperature effect on the hydride transfer.

1-Benzyl-1,4-dihydronicotinamide (BNAH), due to having a very similar structure as NADH, is extensively used as the model of NADH,[4,9,29] and many experiments have shown that BNAH can form a charge-transfer complex with some suitable substrates before the complete hydride transfer,[30] which indicates that the negative kinetic temperature effect on the hydride transfer from NADH and its close analogue BNAH could occur. In this paper, we used BNAH as the NADH model and the radical cation of *N*-benzylphenothiazine ($PTZ^{\bullet+}$)[31] as the hydride acceptor to examine the kinetic temperature effect on the hydride transfer from BNAH to $PTZ^{\bullet+}$. As a result, a significant negative kinetic temperature effect on the hydride transfer from BNAH to $PTZ^{\bullet+}$ was observed.

Results and Discussion

Reaction of G-BNAH with $PTZ^{\bullet+}$ and the Negative Kinetic Temperature Effect. The radical cation of *N*-benzylphenothi-

(3) (a) Zielonka, J.; Marcinek, A.; Adamus, J.; Gebicki, J. *J. Phys. Chem. A.* **2003**, *107*, 9860. (b) Marcinek, A.; Rogowski, J.; Adamus, J.; Gebicki, J.; Bednarek, P.; Bally, T. *J. Phys. Chem. A* **2000**, *104*, 718. (c) Marcinek, A.; Adamus, J.; Huben, K.; Gebicki, J.; Bartczak, T. J.; Bednarek, P.; Bally, T. *J. Am. Chem. Soc.* **2000**, *122*, 437. (d) Gebicki, J.; Marcinek, A.; Zielonka, J. *Acc. Chem. Res.* **2004**, *37*, 379.

(4) (a) Fukuzumi, S.; Inada, O.; Suenobu, T. *J. Am. Chem. Soc.* **2003**, *125*, 4808. (b) Fukuzumi, S.; Inada, O.; Suenobu, T. *J. Am. Chem. Soc.* **2002**, *124*, 14538.

(5) (a) Powell, F.; Wu, S. C.; Bruice, T. C. *J. Am. Chem. Soc.* **1984**, *106*, 3850. (b) Carlson, B. W.; Miller, L. L. *J. Am. Chem. Soc.* **1983**, *105*, 7453. (c) Fukuzumi, S.; Koumitsu, S.; Hironaka, K.; Tanaka, T. *J. Am. Chem. Soc.* **1987**, *109*, 305. (d) Sinha, A.; Bruice, T. C. *J. Am. Chem. Soc.* **1984**, *106*, 7291. (e) Carlson, B. W.; Miller, L. L.; Neta, P.; Gradkowski, J. *J. Am. Chem. Soc.* **1984**, *106*, 7233. (f) Lai, C. C.; Colter, A. K. *J. Chem. Soc., Chem. Commun.* **1980**, 1115.

(6) Lo, H. C.; Fish, R. H. *Angew. Chem., Int. Ed.* **2002**, *41*, 478.

(7) (a) Lee, I.-S. H.; Chow, K.-H.; Kreevoy, M. M. *J. Am. Chem. Soc.* **2002**, *124*, 7755. (b) Matsuo, T.; Mayer, J. M. *Inorg. Chem.* **2005**, *44*, 2150.

(8) (a) Ellis, W. W.; Raebiger, J. W.; Curtis, C. J.; Bruno, J. W.; DuBois, D. L. *J. Am. Chem. Soc.* **2004**, *126*, 2738. (b) Reichenbach-Klinke, R.; Kruppa, M.; Konig, B. *J. Am. Chem. Soc.* **2002**, *124*, 12999. (c) Bartlett, P. N.; Simon, E. *J. Am. Chem. Soc.* **2003**, *125*, 4014.

(9) (a) Zhu, X.-Q.; Yang, Y.; Zhang, M.; Cheng, J.-P. *J. Am. Chem. Soc.* **2003**, *125*, 15298. (b) Zhu, X.-Q.; Li, H.-R.; Li, Q.; Ai, T.; Lu, J.-Y.; Yang, Y.; Cheng, J.-P. *Chem. Eur. J.* **2003**, *9*, 871. (c) Zhu, X.-Q.; Cao, L.; Liu, Y.; Yang, Y.; Lu, J.-Y.; Wang, J.-S.; Cheng, J.-P. *Chem. Eur. J.* **2003**, *9*, 3937. (d) Zhang, B.-L.; Zhu, X.-Q.; Lu, J.-Y.; He, J.-Q.; Wang, P. G.; Cheng, J.-P. *J. Org. Chem.* **2003**, *68*, 3295.

(10) Buck, H. *Intl. J. Quantum Chem.* **2005**, 101, 389.

(11) Brown, T. L.; LeMay, H. E., Jr.; Bursten, B. E. *Chemistry*: *The Central Science*, 7th ed.; Prentice Hall, 1997; Chapter 14.

(12) Kiselev, V. D.; Miller, J. G. *J. Am. Chem. Soc.* **1975**, *97*, 4036.

(13) (a) Braddock, J. N.; Meyer, T. J. *J. Am. Chem. Soc.* **1973**, *75*, 3158. (b) Braddock, J. N.; Cramer, J. L.; Meyer, T. J. *J. Am. Chem. Soc.* **1975**, *97*, 1972. (c) Cramer, J. L.; Meyer, T. J. *Inorg. Chem.* **1974**, *13*, 1250.

(14) Sutin, N.; Gordon, B. M. *J. Am. Chem. Soc.* **1961**, *83*, 70.

(15) (a) Yoder, J. C.; Roth, J. P.; Gussenhoven, E. M.; Larsen, A. S.; Mayer, J. M. *J. Am. Chem. Soc.* **2003**, *125*, 2629. (b) Mader, E. A.; Larsen, A. S.; Mayer, J. M. *J. Am. Chem. Soc.* **2004**, *126*, 8066.

(16) Fukuzumi, S.; Endo, Y.; Imahori, H. *J. Am. Chem. Soc.* **2002**, *124*, 10974.

(17) Frank, R.; Greiner, G.; Rau, H. *Phys. Chem. Chem. Phys.* **1999**, *1*, 3481.

(18) Fukuzumi, S.; Ohkubo, K. *J. Phys. Chem. A* **2005**, *109*, 1105.

(19) (a) Mozurkewich, M.; Lamb, J. J.; Benson, S. W. *J. Phys. Chem.* **1984**, *88*, 6435. (b) Lamb, J. J.; Mozurkewich, M.; Benson, S. W. *J. Phys. Chem.* **1984**, *88*, 6441. (c) Sen Sharma, D. K.; Kebarle, P. *J. Am. Chem. Soc.* **1982**, *104*, 19. (d) Menon, A.; Sthyamurthy, N. *J. Phys. Chem.* **1981**, *85*, 1021. (e) Meot-Ner(Mautner), M.; Field, F. H. *J. Am. Chem. Soc.* **1978**, *100*, 1356. (f) Hiatt, R.; Benson, S. W. *J. Am. Chem. Soc.* **1972**, *94*, 6886. (g) Connor, J.; Roodselaar, A. V.; Fair, R. W.; Strausz, O. P. *J. Am. Chem. Soc.* **1971**, *93*, 560.

(20) (a) Kim, H.-B.; Kitamura, N.; Kawanishi, Y.; Tazuke, S. *J. Am. Chem. Soc.* **1987**, *109*, 2506. (b) Kitamura, N.; Obata, R.; Kim, H.-B.; Tazuke, S. *J. Phys. Chem.* **1987**, *91*, 2033. (c) Kim, H.-B.; Kitamura, N.; Kawanishi, Y.; Tazuke, S. *J. Phys. Chem.* **1989**, *93*, 5757. (d) Kitamura, N.; Obata, R.; Kim, H.-B.; Tazuke, S. *J. Phys. Chem.* **1989**, *93*, 5764.

(21) (a) Olson, J. B.; Koch, T. H. *J. Am. Chem. Soc.* **1986**, *108*, 756. (b) Wang, J.; Doubleday: C. J.; Turro, N. J. *J. Am. Chem. Soc.* **1989**, *111*, 3962.

(22) Kapinus, E. I.; Rau, H. *J. Phys. Chem. A* **1998**, *102*, 5569.

(23) (a) Moss, R. A.; Lawrynowicz, W.; Turro, N. J.; Gould, I. R.; Cha, Y. *J. Am. Chem. Soc.* **1986**, *108*, 7028. (b) Turro, N. J.; Lehr, G. F.; Butcher, J. A.; Moss, R. A.; Guo, W. *J. Am. Chem. Soc.* **1982**, *104*, 1754.

(24) (a) Shimomura, T.; Tölle, K. J.; Smid, J.; Szwarc, M. *J. Am. Chem. Soc.* **1967**, *89*, 796. (b) Murphy, R. B.; Libby, W. F. *J. Am. Chem. Soc.* **1977**, *99*, 39. (c) Albrecht-Gary, A.-M.; Dietrich-Buchecker, C.; Saad, Z.; Sauvage, J.-P. *J. Chem. Soc., Chem. Commun.* **1992**, 280. (d) Fernado, S. R. L.; Maharoof, U. S. M.; Deshayes, K. D.; Kinstle, T. H.; Ogawa, M. Y. *J. Am. Chem. Soc.* **1996**, *118*, 5783.

(25) Reitstöen, B.; Parker, V. D. *J. Am. Chem. Soc.* **1990**, *112*, 4968.

(26) Yamamoto, S.; Sakurai, T.; Yingjin, L.; Sueishi, Y. *Phys. Chem. Chem. Phys.* **1999**, *1*, 833.

(27) Zaman, K. M.; Yamamoto, S.; Nishimura, N.; Maruta, J.; Fukuzumi, S. *J. Am. Chem. Soc.* **1994**, *116*, 12099.

(28) Fukuzumi, S.; Ohkubo, K.; Tokuda, Y.; Suenobu, T. *J. Am. Chem. Soc.* **2000**, *122*, 4286.

(29) (a) Kobayashi, A.; Konno, H.; Sakamoto, K.; Sekine, A.; Ohashi, Y.; Iida, M.; Ishitani, O. *Chem. Eur. J.* **2005**, *11*, 4219. (b) Watanabe, S.; Kosaka, N.; Kondo, S.; Yano, Y. *Bull. Chem. Soc. Jpn.* **2004**, *77*, 569. (c) Fukuzumi, S.; Fyujii, Y.; Suenobu, T. *J. Am. Chem. Soc.* **2001**, *123*, 10191. (d) Moriya, H.; Kajiki, T.; Watanabe, S.; Kondo, S.; Yano, Y. *Bull. Chem. Soc. Jpn.* **2000**, *73*, 2539. (e) Liu, Y.-C.; Li, X.-Z.; Yang, C.; Guo, Q.-X. *Bioorg. Chem.* **2001**, *29*, 14. (f) Lu, Y.; Xian, M.; Cheng, J.-P.; Xia, C.-Z. *Acta Chim. Sin.* **1997**, *55*, 1145.

(30) (a) Fukuzumi, S.; Nishizawa, N.; Tanaka, T. *J. Org. Chem.* **1984**, *49*, 3571. (b) Hajdu, J.; Sigman, D. S. *J. Am. Chem. Soc.* **1976**, *98*, 6060.

(31) (a) Mitchell, P. *Aust. N. Z. J. Psych.* **1993**, *27*, 370. (b) Gooley, C. M.; Keyzer, H.; Setchell, F. *Nature* **1969**, *223*, 81. (c) Ohnishi, S.; McConnell, H. M. *J. Am. Chem. Soc.* **1965**, *87*, 2293.

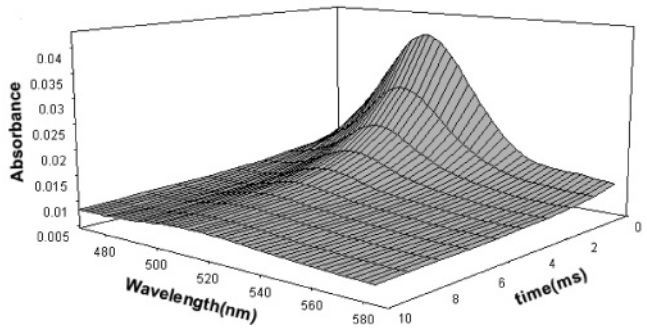

FIGURE 1. Stack plot of spectra for the reaction of BNAH (1.0×10^{-4} M) with the radical cation of *N*-benzylphenothiazine ($PTZ^{\bullet+}$) (1.0×10^{-4} M) in acetonitrile at 298 K.

azine ($PTZ^{\bullet+}$) and 1-(*p*-substituted benzyl)-1,4-dihydronicotinamide (G-BNAH; G = CH_3O, CH_3, H, Cl, Br) were synthesized according to literature methods.[32,33] When G-BNAH was treated by the radical cation of *N*-benzylphenothiazine ($PTZ^{\bullet+}$) in acetonitrile at room temperature, the corresponding compounds—G-BNA^+, *N*-benylphenothiazine (PTZ), and $PTZH^+$—were obtained as the final products, which clearly shows that during the reaction process, G-BNAH released a hydride ion. The spectrophotometric titration experiments suggest that 2 mol of $PTZ^{\bullet+}$ were required to consume 1 mol of G-BNAH completely (eq 1, Figure S1). The reaction rate was determined

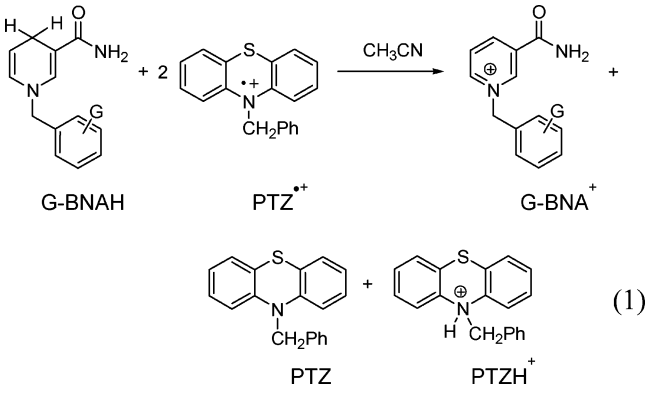

(1)

with an Applied Photophysics SX.18MV-R stopped-flow spectrometer by monitoring the spectra change of $PTZ^{\bullet+}$ (Figure 1). The second order observed rate constants (k_{obs}) for the reaction at different temperatures between 298 and 318K are listed in Table 1. The activation parameters of the reaction—activation enthalpy ($\Delta H^{\ddagger}_{obs}$) and activation entropy ($\Delta S^{\ddagger}_{obs}$)—were derived from the Eyring plots of $\ln(k_{obs}/T)$ versus the reciprocal of the absolute temperature ($1/T$),[34] which were listed in Table 3.

From Table 1, it is clear that the most striking feature of the reaction of G-BNAH with $PTZ^{\bullet+}$ is that as the reaction temperature increases from 298 to 318 K, the reaction rates (k_{obs}) decreased rather than increased and the negative kinetic temperature effect on the reaction rates (meaning "*the lower the temperature, the faster the reaction rate*"[28]) increased as the

TABLE 1. Second-Order Observed Rate Constants (k_{obs}) for the Reaction of G-BNAH with $PTZ^{\bullet+}$ in Deaerated Acetonitrile at Various Temperatures

	$k_{obs} \times 10^{-7}$ (M^{-1} s^{-1})[a]				
G-BNAH	298 K	303 K	308 K	313 K	318 K
p-OCH_3	3.49	3.19	3.01	2.73	2.60
p-CH_3	3.16	2.87	2.72	2.58	2.33
p-H	2.80	2.60	2.50	2.27	2.16
p-Cl	2.10	1.99	1.89	1.73	1.66
p-Br	2.13	2.01	1.90	1.75	1.68

[a] The experimental errors are within ±5%.

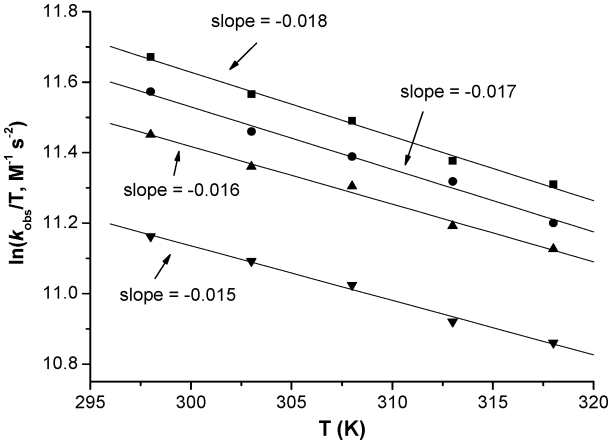

FIGURE 2. The plots of $\ln(k_{obs}/T)$ against the reaction temperature (K) for the reaction of $PTZ^{\bullet+}$ with CH_3O−BNAH (■), CH_3−BNAH (●), BNAH (▲), and Cl−BNAH (▼) in acetonitrile.

substituent (G) on the benzyl ring of G-BNAH was going from the electron-withdrawing group (G = Br) to the electron-donating group (G = OCH_3) (Figure 2). By examining the activation parameters of the reactions, it is found that the activation enthalpies ($\Delta H^{\ddagger}_{obs}$) all were negative, and the negative values increased as the substituent was going from the electron-withdrawing group to the electron-donating group (from −2.9 kcal/mol for *p*-Br to −3.4 kcal/mol for *p*-OCH_3). To our best knowledge, this is the first time the negative kinetic temperature dependence of rate in the hydride transfer mediated by the NADH model BNAH has been observed. Since the Hammett reaction constant ρ for the reaction is a negative value (ρ = −0.436) (see Figure 3) and the logarithmic values of k_{obs} are strongly dependent on the standard oxidation potentials of G-BNAH (Figure 4), it is conceived that charge transfer, electron transfer, or hydride transfer from G-BNAH to $PTZ^{\bullet+}$ would be in the rate-determining step of the reaction.

According to the negative activation enthalpies ($\Delta H^{\ddagger}_{obs}$) for the reactions of G-BNAH with $PTZ^{\bullet+}$, it is conceivable that between the reactant pair (G-BNAH and $PTZ^{\bullet+}$) and the transition state of the reactions would exist a CT-complex as the reaction intermediate,[12−28,35] and the state energy of the CT-complex should be not only smaller than that of the reactant pair, but also smaller than that of the transition state of the reactions. So, to determine the origin resulting in the negative kinetic temperature effect on the reaction of G-BNAH with $PTZ^{\bullet+}$, it is necessary to examine and determine the CT-complex formed between G-BNAH and $PTZ^{\bullet+}$ during the reaction process.

(32) Mauserall, D.; Westheimer, F. H. *J. Am. Chem. Soc.* **1955**, *77*, 2261.
(33) (a) Clarke, D.; Gilbert, B. C.; Hanson, P.; Kirk, C. M. *J. Chem. Soc., Perkin Trans. 2* **1978**, 1103−1110. (b) Apreda, M. C.; Cano, F. H.; Foces-Foces, C.; López-Rupérez, F.; Jose, C. *J. Chem. Soc., Perkin Trans. 2* **1987**, 575−579.
(34) Wei, Y.-Y.; Li, J. *Hua Xue Fan Ying Ji Li Dao Lun*; Ke Xue Chu Ban She, 2004; p 27.
(35) Lu, Y.; Zhao, Y.-X.; Handoo, K. L.; Parker, V. D. *Org. Biomol. Chem.* **2003**, *1*, 173.

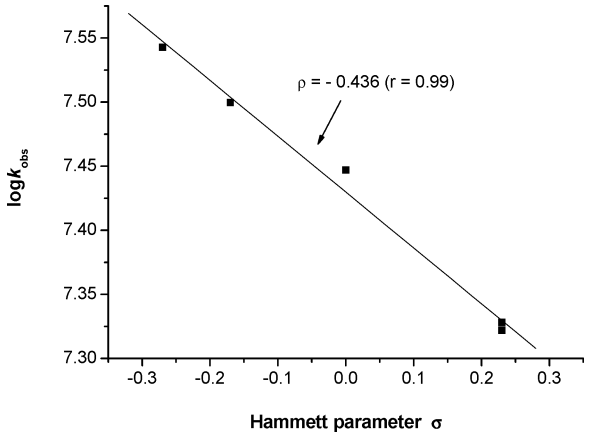

FIGURE 3. Correlation of log k_{obs} (at 298 K) versus Hammett substituent constants σ for the reaction of G-BNAH with PTZ$^{\bullet+}$.

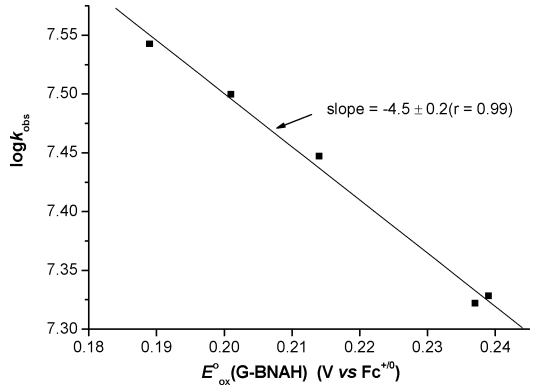

FIGURE 4. Correlation of log k_{obs} (at 298 K) versus the standard oxidation potentials of G-BNAH.

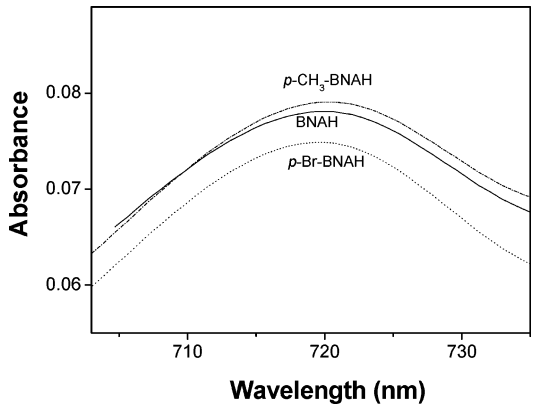

FIGURE 5. Visible−UV spectra of the CT-complex of G-BNAH (3.0×10^{-4} M) with the radical cation of *N*-benzylphenothiazine (PTZ$^{\bullet+}$) (3.0×10^{-4} M) in acetonitrile at 298 K.

CT-Complex Formed between G-BNAH and PTZ$^{\bullet+}$. When BNAH and PTZ$^{\bullet+}$ were mixed in acetonitrile, a new broad absorption band at $\lambda_{max} = 720$ nm, which is the characteristic of a CT-complex, is immediately observed (Figure 5). Since neither BNAH nor PTZ$^{\bullet+}$ has absorption at this absorption range and BNAH can form a CT-complex with many suitable substrates before the hydride complete transfer, the new broad absorption band should originate from the CT-complex formed between G-BNAH and PTZ$^{\bullet+}$ (Figure 5).[30] The equilibrium constant (K_{CT}) of the CT-complex was estimated from the initial absorbance of the CT-complex by changing the concentrations of G-BNAH according to the Benesi−Hildebrand equation (eq 2).[36] The values of the equilibrium constant (K_{CT}) at different temperatures from 298 to 318K are summarized in Table 2. The corresponding thermodynamic parameters for the CT-complex formation were obtained from the plots of ln K_{CT} vs $1/T$ according to the van't Hoff equation,[37] which are listed in Table 3.

TABLE 2. Equilibrium Constants for the Formation of the CT-Complexes of G-BNAH with PTZ$^{\bullet+}$ in Deaerated Acetonitrile at Various Temperatures

G-BNAH	λ_{max} (nm) of CT-complex	$K_{CT} \times 10^{-3}$ (M^{-1})[a] 298 K	303 K	308 K	313 K	318 K
p-OCH_3	722	3.9	3.4	2.7	2.4	2.0
p-CH_3	722	3.7	3.2	2.6	2.3	1.9
p-H	720	3.4	2.9	2.5	2.0	1.8
p-Cl	719	3.3	2.7	2.3	2.0	1.7
p-Br	718	3.2	2.8	2.3	2.0	1.7

[a] The uncertainties are not larger than ±7%.

TABLE 3. Standard Formation Enthalpy and Entropy Changes of CT-Complex Formed between G-BNAH and PTZ$^{\bullet+}$, Activation Parameters of the CT-Complex, and the Eyring Activation Parameters of the Reaction of G-BNAH and PTZ$^{\bullet+}$ in Acetonitrile

G-BNAH	$\Delta H°_{CT}$[a]	$\Delta S°_{CT}$[b]	$\Delta H^{\ddagger}_{H-T}$[a]	$\Delta S^{\ddagger}_{H-T}$[b]	$\Delta H^{\ddagger}_{obs}$[a]	$\Delta S^{\ddagger}_{obs}$[b]
p-OCH_3	−6.4	−5.1	3.0	−30.5	−3.4	−35.6
p-CH_3	−6.3	−4.7	3.0	−30.8	−3.3	−35.5
p-H	−6.2	−4.6	3.1	−30.3	−3.1	−34.9
p-Cl	−6.0	−4.1	3.1	−30.8	−2.9	−34.9
p-Br	−6.0	−4.1	3.1	−30.7	−2.9	−34.8

[a] Units of kcal·mol^{-1}. [b] Units of cal K^{-1} mol^{-1}.

$$[PTZ^{\bullet+}]/A = 1/(K_{CT}\epsilon[\text{G-BNAH}]) + 1/\epsilon \qquad (2)^{38}$$

From Figure 5 and Table 2, it is clear that before the hydride transfer from G-BNAH to PTZ$^{\bullet+}$, a CT-complex was formed between G-BNAH and PTZ$^{\bullet+}$. The value scale of the standard formation enthalpy of the CT-complex ranges from −6.4 kcal/mol for G-BNAH (G = CH_3O) to −6.0 kcal/mol for G-BNAH (G = Br). Since the negative values of the standard formation enthalpy of the CT-complex are increased from the electron-withdrawing group (G = Br) to the electron-donating group (G = OCH_3), the CT-complex could be constructed by charge transfer from G-BNAH to PTZ$^{\bullet+}$.[26−28] In terms of the relationship that the observed activation enthalpy $\Delta H^{\ddagger}_{obs}$ for the reaction of G-BNAH with PTZ$^{\bullet+}$ is equal to the combination of the formation enthalpy of the CT-complex ($\Delta H°_{CT}$) (always negative values) and the activation enthalpy of the CT-complex to reach the transition state ($\Delta H^{\ddagger}_{H-T}$) (eq 3),[15,18,26,27] the activation enthalpy of the CT-complex to reach the transition state ($\Delta H^{\ddagger}_{H-T}$) can be easily derived from eq 3, and the results were summarized in Table 3.

$$\Delta H^{\ddagger}_{obs} = \Delta H°_{CT} + \Delta H^{\ddagger}_{H-T} \qquad (3)$$

From Table 3, it is clear that $\Delta H^{\ddagger}_{H-T}$ is positive, but $\Delta H°_{CT}$ is negative. The increase of the reaction temperature is favorable

(36) Benesi, H. A.; Hildebrand, J. H. *J. Am. Chem. Soc.* **1949**, *71*, 2703.
(37) Song, H.-C. *J. Zhengzhou Institute Light Ind.* **1995**, *10*, 1.
(38) A = absorbance at λ_{max} of the CT-complex; K_{CT} = equilibrium constants for CT-complex formation; ϵ = extinction coefficient.

SCHEME 1. Possible Mechanisms for the Reaction of G-BNAH with PTZ$^{\bullet+}$ in Acetonitrile

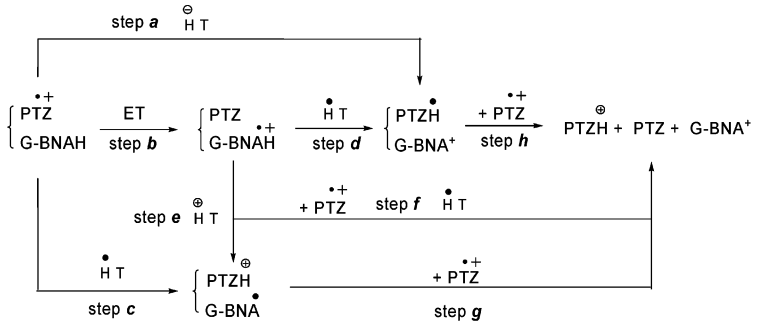

$$\text{step } \boldsymbol{a}: \quad \Delta H(\boldsymbol{a}) = \Delta H_{rxn} - F[E^{o}(PTZH^{+/0}) - E_{1/2}(PTZ^{+/0})] \tag{4}$$

$$\text{step } \boldsymbol{b}: \quad \Delta G(\boldsymbol{b}) = -F[E_{1/2}(PTZ^{+/0}) - E^{o}(G\text{-}BNAH^{+/0})] \tag{5}$$

$$\text{step } \boldsymbol{c}: \quad \Delta H(\boldsymbol{c}) = \Delta H_{rxn} - F[E^{o}(G\text{-}BNA^{+/0}) - E_{1/2}(PTZ^{+/0})] \tag{6}$$

$$\text{step } \boldsymbol{d}: \quad \Delta H(\boldsymbol{d}) = \Delta H_{rxn} - F[E^{o}(G\text{-}BNAH^{+/0}) - E_{1/2}(PTZ^{+/0})] - F[E^{o}(PTZH^{+/0}) - E_{1/2}(PTZ^{+/0})] \tag{7}$$

$$\text{step } \boldsymbol{e}: \quad \Delta H(\boldsymbol{e}) = \Delta H_{rxn} - F[E^{o}(G\text{-}BNAH^{+/0}) - E_{1/2}(PTZ^{+/0})] - F[E^{o}(G\text{-}BNA^{+/0}) - E_{1/2}(PTZ^{+/0})] \tag{8}$$

$$\text{step } \boldsymbol{f}: \quad \Delta H(\boldsymbol{f}) = \Delta H_{rxn} - F[E^{o}(G\text{-}BNAH^{+/0}) - E_{1/2}(PTZ^{+/0})] \tag{9}$$

$$\text{step } \boldsymbol{g}: \quad \Delta G(\boldsymbol{g}) = -F[E_{1/2}(PTZ^{+/0}) - E^{o}(G\text{-}BNA^{+/0})] \tag{10}$$

$$\text{step } \boldsymbol{h}: \quad \Delta G(\boldsymbol{h}) = -F[E_{1/2}(PTZ^{+/0}) - E^{o}(PTZH^{+/0})] \tag{11}$$

to the activation of the formed CT-complex, but unfavorable to the formation of the CT-complex at the same time. Since the absolute value of ΔH°_{CT} is larger than the value of $\Delta H^{\ddagger}_{H-T}$, the temperature factor has a larger effect on the formation of the CT-complex than on the activation of the formed CT-complex, which resulted in the abnormal experimental situation for the reaction of G-BNAH with PTZ$^{\bullet+}$ in acetonitrile that *the higher the temperature, the slower the reaction.*

Mechanism and Thermodynamics of the Reaction of G-BNAH with PTZ$^{\bullet+}$. From the previous studies,[26−28] it appeared that the negative temperature effects on the hydride transfer from organic hydrides (such as Michler's hydride and 9-substituted 10-methyl-9,10-dihydroacridine) all were thought to occur in the initial single-electron-transfer step. No paper was found to report the negative temperature effect that occurred in the concerted hydride transfer process. As to the present reaction that also has a negative temperature effect, whether or not the hydride transfer from G-BNAH to PTZ$^{\bullet+}$ also was initiated by single electron transfer is the question. To thoroughly elucidate the practice pathway of the reaction, the detailed **thermodynamics** of each mechanistic step for the hydride transfer from G-BNAH to PTZ$^{\bullet+}$ needs to be obtained. According to the typical chemical properties of G-BNAH and PTZ$^{\bullet+}$ as well as the reaction final products (eq 1), five possible pathways can be proposed for the practice mechanism of the hydride transfer from G-BNAH to PTZ$^{\bullet+}$ as shown in Scheme 1 (i.e., the paths of a−h; b−d−h; b−f; b−e−g; and c−g). In the path a−h, the hydride transfer from G-BNAH to PTZ$^{\bullet+}$ was completed by direct one-step transfer mechanism to form G-BNA^{+} and PTZH$^{\bullet}$, and the latter was then oxidized by another PTZ$^{\bullet+}$ to yield the final products (PTZH^{+} and PTZ). In the paths b−d−h, b−f, and b−e−g, the hydride transfer was initiated by single electron transfer from G-BNAH to PTZ$^{\bullet+}$ to form G-BNAH$^{\bullet+}$ and PTZ, but the second reaction step among the three pathways is different: the second reaction step for the path b−d−h is hydrogen atom transfer from G-BNAH$^{\bullet+}$ to PTZ to become G-BNA^{+} to PTZH$^{\bullet}$, the latter was then oxidized by another PTZ$^{\bullet+}$ to yield the final products; the second reaction step for the path b−f is hydrogen atom transfer from G-BNAH$^{\bullet+}$ to another PTZ$^{\bullet+}$ to form the final reaction products; and the second reaction step for the path b−e−g is proton transfer from G-BNAH$^{\bullet+}$ to PTZ to become PTZH^{+} and G-BNA$^{\bullet}$, and the latter was then oxidized by another PTZ$^{\bullet+}$ to yield the final products. In the path c−g, the hydride transfer was initiated by neutral hydrogen atom transfer from G-BNAH to PTZ$^{\bullet+}$ to form PTZH^{+} and G-BNA$^{\bullet}$, and the latter was then oxidized by another PTZ$^{\bullet+}$ to yield the final products. It is clear that all five pathways give the same final reaction products. It follows that an interesting but difficult question is produced: which one is the practical pathway of the hydride transfer from G-BNAH to PTZ$^{\bullet+}$. Obviously, it is necessary to access the thermodynamic data of each mechanistic step for the hydride transfer from G-BNAH to PTZ$^{\bullet+}$ to determine the practical pathway of the hydride transfer from G-BNAH to PTZ$^{\bullet+}$.

To estimate the standard state enthalpy change of each mechanistic step, eight equations (4−11)[39] were developed, in which eqs 4, 6, 7, 8, and 9 were derived from five suitable thermodynamic cycles (Schemes S1−S5 in the Supporting Information) according to Hess' law (where $F = 23.06$ kcal mol^{-1} V^{-1} is the Faraday constant), from which the change of the standard state enthalpy or standard state free energy for each elementary step shown in Scheme 1 can be easily derived only if the enthalpy change of the reaction (eq 1) and the standard redox potentials of the related species are available. Evidently, the enthalpy changes of reaction 1 (ΔH_{rxn}) can be obtained from the corresponding reaction heat, which can be directly determined by titration calorimetery (Figure 6). The standard redox

(39) It should be pointed out herein that we used the term free energy change ΔG_{eT} to replace the enthalpy change ΔH_{eT} for the electron-transfer processes. The validation of using free energy change ΔG_{eT} instead of enthalpy change ΔH_{eT} for electron-transfer processes is that entropies associated with electron transfer are negligible, and ΔG_{eT} can be combined directly with ΔH_{eT}, which has been verified by Arnett's work: Arnett, E. M.; Amarnath, K.; Harvey, N. G.; Cheng, J.-P. *J. Am. Chem. Soc.* **1990**, *112*, 2, 344.

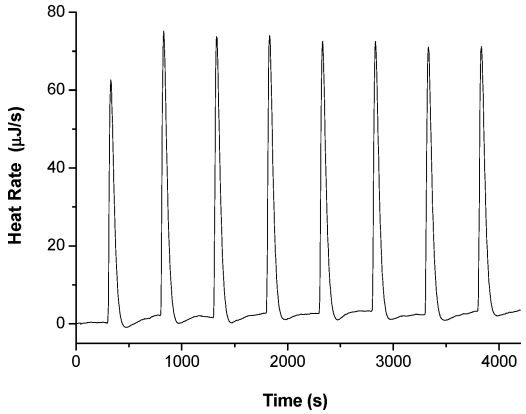

FIGURE 6. Isothermal titration calorimettry (ITC) for the reaction of BNAH with $PTZ^{\bullet+}$ in acetonitrile at 298 K. Titration was conducted by adding 10 μL of BNAH (1.89 mM) every 500 s into the acetonitrile solution containing $PTZ^{\bullet+}ClO_4^-$ (5.01 mM).

TABLE 4. Reaction Enthalpy Changes of the Reactions of G-BNAH with $PTZ^{\bullet+}$ in Acetonitrile (kcal/mol), along with the Redox Potentials of Relative Species in Acetonitrile (V vs $Fc^{+/0}$)

G-BNAH	ΔH_{rxn}[a]	$E_{1/2}$ ($PTZ^{+/0}$)[b]	$E°$ (G-$BNAH^{+/0}$)[c]	$E°$ (G-$BNA^{+/0}$)[c]	$E°$ ($PTZH^{+/0}$)[c]
p-OMe	−43.0	0.334	0.189	−1.209	−1.214
p-CH_3	−42.7	0.334	0.201	−1.168	−1.214
p−H	−42.4	0.334	0.214	−1.156	−1.214
p-Cl	−41.9	0.334	0.237	−1.136	−1.214
p-Br	−41.8	0.334	0.239	−1.135	−1.214

[a] Measured in acetonitrile solution at 298 K in kcal/mol by titration calorimetry. The data given were the average values of at least two independent runs, each of which was again an average value of at least 7 consecutive titrations. The reproducibility was ≤1.0 kcal/mol. [b] Measured in acetonitrile solution at 298 K in volts by the CV method vs ferrocenium/ferrocene redox couple. Reproducible to 5 mV or better. [c] Measured by OSWV and SHACV methods in acetonitrile solution at 298 K in volts vs ferrocenium/ferrocene redox couple. See ref 40.

potentials can be measured by cyclic voltammetry (CV), Osteryoung square wave voltammetry (OSWV), and second-harmonic ac voltammetry (SHACV)[40] (Figure S2−S4). The detailed experimental results were summarized in Table 4, respectively. The thermodynamic data of each mechanistic step shown in Scheme 1 are summarized in Table 5.

From Table 5, it is easy to find that the value scales of the state energy changes for the three initial steps (steps a, b, and c) in the five possible pathways (see Scheme 1) range from −7.3 to −6.1 kcal/mol for the concerted hydride transfer process (step a), from −3.3 to −2.2 kcal/mol for the electron transfer (step b), and from −8.1 to −7.4 kcal/mol for the hydrogen transfer (step c). Since the state energy change for the hydrogen atom transfer is more negative than that for the hydride transfer and for the electron transfer, respectively, step c should be more favorable than the other two possible initial steps to take place. But, according to the strong dependence of the reaction rate of G-BNAH with $PTZ^{\bullet+}$ on Hammett substituent constant σ (ρ = − 0.436) (see Figure 3) and on the standard oxidation potentials of G-BNAH (the line slope is −4.5, see Figure 4), it is reasonable to conclude that the initial hydrogen atom transfer from G-BNAH to $PTZ^{\bullet+}$ (step c) should be ruled out as the initial step for the reaction of G-BNAH with $PTZ^{\bullet+}$.

Concerning steps a and b, a comparison of the state energy changes of the two initial reaction steps (step a and b) with the corresponding observed activation enthalpy changes of the reactions ($\Delta H^{\ddagger}_{obs}$) clearly shows that the observed activation enthalpy changes ($\Delta H^{\ddagger}_{obs}$) (−3.8 to −2.7 kcal/mol) are more negative than the corresponding standard state energy changes of the electron transfer in step b (−3.3 to −2.2 kcal/mol), but less negative than the concerted hydride transfer process in step a (−7.3 to −6.1 kcal/mol). On the basis of a general ***reaction law*** that the activation energy change is always larger than or at least equal to the corresponding standard state free energy change for any elemental reaction,[41] it is evident that step b should be ruled out as the initial reaction, and the only remaining step a should be suitable for the reaction law, i.e., the reaction of G-BNAH with $PTZ^{\bullet+}$ was initiated by the concerted hydride transfer rather than by one-electron or hydrogen atom transfer, even though $PTZ^{\bullet+}$ was generally regarded as a typical one-electron oxidant (Figure 7). These results unambiguously support that the practical mechanism of the hydride transfer from G-BNAH to $PTZ^{\bullet+}$ is the path of steps a−h, i.e., the hydride transfer from G-BNAH to $PTZ^{\bullet+}$ was completed by a direct

TABLE 5. Energetics of Each Mechanistic Step Shown in Scheme 1 (kcal/mol)[a]

	$\Delta H°$ (or $\Delta G°$)							
G-BNAH	step a	step b	step c	step d	step e	step f	step g	step h
CH_3O	−7.3	−3.3	−7.4	−4.0	−4.1	−39.6	−35.6	−35.7
CH_3	−7.0	−3.1	−8.1	−3.9	−5.0	−39.6	−34.6	−35.7
H	−6.7	−2.8	−8.0	−3.9	−5.3	−39.6	−34.4	−35.7
Cl	−6.2	−2.2	−8.0	−4.0	−5.8	−39.7	−33.9	−35.7
Br	−6.1	−2.2	−7.9	−3.9	−5.7	−39.6	−33.9	−35.7

[a] The enthalpy changes calculated from eqs 4 and 6−9 for step a and c−f are the combinations of enthalpy and free energy terms. The free energy for the electron transfer $\Delta G°$ to replace the enthalpies changes $\Delta H°$ is reasonable. See ref 39.

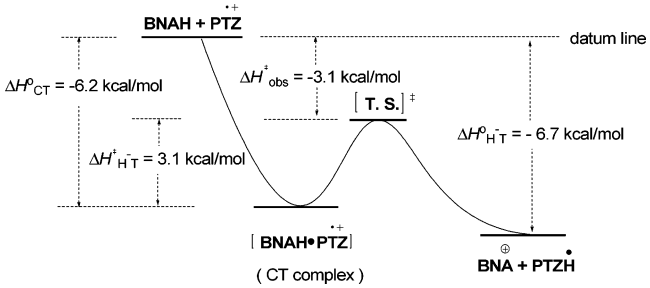

FIGURE 7. Coordinate diagram of the electron transfer from BNAH to $PTZ^{+\bullet}$ in acetonitrile.

(40) The SHACV and OSWV methods provide superior approaches to directly evaluating the one-electron redox potentials in the presence of a follow-up chemical reaction and it is regarded that both phase selective ac and square wave techniques are powerful in studying irreversible or nearly irreversible systems. See: (a) Bard, A. J.; Faulkner, L. R. *Electrochemical Methods, Fundamental and Applications*; John Wiley & Sons: New York, 2001; Chapter 10, pp 368−416. (b) McCord, T. G.; Smith, D. E. *Anal. Chem.* **1969**, *41*, 1423. (c) Bond, A. M.; Smith, D. E. *Anal. Chem.* **1974**, *46*, 1946. (d) Wasielewski, M. R.; Breslow, R. *J. Am. Chem. Soc.* **1976**, *98*, 4222. (e) Arnett, E. M.; Amarnath, K.; Harvey, N. G.; Cheng, J.-P. *J. Am. Chem. Soc.* **1990**, *112*, 344. (f) Fukuzumi, S.; Nishimine, M.; Ohkubo, K.; Tkachenko, N. V.; Lemmetyinen, H. *J. Phys. Chem. B* **2003**, *107*, 12511. (g) Ofial, A. R.; Ohkubo, K.; Fukuzumi, S.; Lucius, R.; Mayr, H. *J. Am. Chem. Soc.* **2003**, *125*, 10906. (h) Osteryoung, J. G.; Osteryoung. R. A. *Anal. Chem.* **1985**, *57*, 101. (i) Ivaska, A. U.; Smith, E. E. *Anal. Chem.* **1985**, *57*, 1910. (j) O'Dea, J.; Wojciechowski, M.; Osteryoung, J. *Anal. Chem.* **1985**, *57*, 954−955.

(41) (a) Hine, J. *Adv. Phys. Org. Chem.* **1977**, *15*, 1. (b) Page, M.; Williams, A. *Organic and Bio-organic Mechanism*; Addison-Wesley Longman Limited 1997; Chapter 1, pp 1−22.

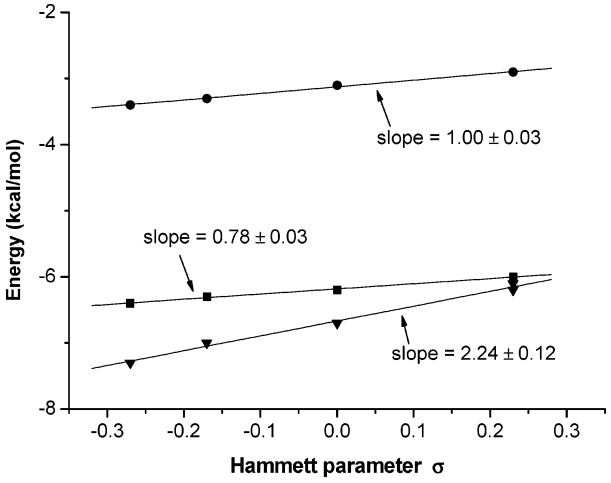

FIGURE 8. Hammett plots of $\Delta H°_{CT}$ (■), $\Delta H^{‡}_{obs}$ (●), and $\Delta H°_{H^-T}$ (▼) vs Hammett substituent constants. The values of $\Delta H°_{CT}$ and $\Delta H^{‡}_{obs}$ are listed in Table 3; the values of $\Delta H°_{H^-T}$ (energies changes of step a) are listed in Table 5, respectively.

one-step mechanism to form G-BNA$^+$ and PTZH$^•$, the latter was then oxidized by another PTZ$^{•+}$ to yield the final products (PTZH$^+$ and PTZ). Considering that the state energy change for the second step (step h) (−35.7 kcal/mol) is much more negative than that for the corresponding initial reaction step (step a), it is conceivable that the hydride transfer in the initial step is the rate-determining step. The coordinate diagram of the concerted hydride transfer from BNAH to PTZ$^{•+}$ via a CT-complex in acetonitrile is shown in Figure 7. Since the structure of G-BNAH is quite closed to the redox active center of NADH and PTZ$^{•+}$ can be generated in the metabolism of phenothiazine-based drug in vivo,[31] the negative kinetic temperature effect observed here in the hydride transfer from G-BNAH to PTZ$^{•+}$ may suggest that a similar phenomenon could also occur in the mammalian body, i.e., when the temperature of the mammalian body increases, the reaction rate of NADH with the radical cation of phenothiazine drug could decrease.

Evaluation of the Effective Charge Distribution on the Pyridine Ring in the Hydride Transfer Process. Although CT-complexes in the NADH mimicing reductions have been observed for a long time, no quantitative estimation about the charge transfer from the pyridine ring in the CT-complexes has been available until now. To quantitatively examine the process details of the hydride transfer from G-BNAH to PTZ$^{•+}$ and further elucidate the electrostatic character of the charge-transfer complex and the transition state of the reaction, the effective charge distribution on the pyridine ring in G-BNAH at the various stages (the reactant G-BNAH, the charge-transfer complex, the transition state, and the product G-BNA$^+$) was estimated by using the method of Hammett-type linear free energy analysis, since the Hammett linear free-energy relationship analysis can provide a very efficient access to estimate the effective charge distribution.[42] Figure 8 shows the plots of the formation enthalpy of the CT-complex ($\Delta H°_{CT}$), the observed activation enthalpy of the reaction of G-BNAH with PTZ$^{•+}$ ($\Delta H^{‡}_{obs}$), and the energy change of hydride transfer from G-BNAH to PTZ$^{•+}$ ($\Delta H°_{H^-T}$) against the Hammett substituent constant σ. From Figure 8, three excellent straight lines with the line slopes of 0.78 ± 0.03 (equivalent to ρ of −0.14)[43] for the formation process of the CT-complex, 1.00 ± 0.03 (equivalent to ρ of −0.18)[43] for the process from the reactants to the transition state, and 2.24 ± 0.12 (equivalent to ρ of −0.39)[43] for the hydride transfer from G-BNAH to PTZ$^{•+}$ are observed, which means that the Hammett linear free energy relationship holds in the three chemical processes. According to the intrinsic property of the Hammett substituent effect, it is conceived that the sign of the line slope values reflects an increase or decrease of the effective charge on the nitrogen (N1) atom in the pyridine ring and the magnitude of the line slope values is a measurement of the effective charge change on the N1 atom during the corresponding reaction processes.[44] To quantitatively evaluate the relative effective charge changes on the N1 atom for the three reaction processes, we defined that the effective charge on the N1 atom in G-BNAH is zero, and the effective charge on the N1 atom in G-BNA$^+$ is a positive one (+1), which is from our basic knowledge of the electronic structures of the neutral G-BNAH and the corresponding quaternary ammonium salts G-BNA$^+$. This definition indicates that the positive line slope of 2.24 for the hydride transfer from G-BNAH to PTZ$^{•+}$ is equivalent to the positive effective charge increase of one unit (+1) on the N1 atom from G-BNAH to G-BNA$^+$. According to this relationship, it is easy to deduce that the line slope of 0.78 for the formation of the CT-complex is equivalent to the positive effective charge increase of 0.35 on the N1 atom from the free G-BNAH as the reactant to the complex state of G-BNAH in the CT-complex.[9b,c,42,45] Since the effective charge on the N1 atom in free G-BNAH has been defined as zero, the effective charge on the N1 atom in the CT-complex should be +0.35 (Scheme 2). Similarly, the slope of 1.00 for the chemical reaction process from the reactants to the transition state should be equivalent to the positive effective charge increase of 0.45 on the N1 atom in going from the free G-BNAH as the reactant to the G-BNAH moiety in the transition state, which indicates that the N1 atom on the pyridine ring in the transition state should possess an effective charge of +0.45. Since the CT-complex was formed by the charge transfer of −0.35 from G-BNAH to PTZ$^{•+}$, the reaction process from the CT-complex to the complete formation of G-BNA$^+$ was performed only by hydrogen atom transfer with partial negative charge (−0.65). The details of the effective charge changes on the N1 atom during the hydride transfer from G-BNAH to PTZ$^{•+}$ is shown in Scheme 2.

From Scheme 2, it is clear that relative to the free G-BNAH, the G-BNAH moiety in the CT-complex carries the effective positive charge of 0.35, which means that the CT-complex was formed by the charge (−0.35) transfer from G-BNAH to PTZ$^{•+}$. Similarly, relative to the free G-BNAH, the G-BNAH moiety in the transition state of the reaction of G-BNAH with PTZ$^{•+}$ carries the effective positive charge of 0.45, which means that the formation of the transition state from the reaction of G-BNAH with PTZ$^{•+}$ was completed by the transfer of 45% hydride ion. To our best knowledge, this is the first time the charge distribution at the stage of CT-complex and the transition

(42) (a) Page, M.; Williams, A. *Organic and Bio-organic Mechanism*; Addison-Wesley Longman Limited: Reading, MA, 1997; Chapter 3, pp52−79. (b) Williams, A. *Acc. Chem. Res.* **1989**, *22*, 387. (c) Williams, A. *J. Am. Chem. Soc.* **1985**, *107*, 6335.

(43) According to Hammett equation log $K = \rho\sigma$ and $\Delta H \approx -RT$ log K, the line slope of ΔH against σ should be approximately equal to -5.7ρ. See more in refs 9b, 9c and 45.

(44) Isaacs, N. S. *Physical Organic Chemistry*, 2nd ed.; John Wiley & Sons: New York, 1995; Chapter 4, p 161.

(45) (a) Zhu, X.-Q.; Hao, W.-F.; Tang, H.; Wang, C.-H.; Cheng, J.-P. *J. Am. Chem. Soc.* **2005**, *127*, 2696. (b) Zhu, X.-Q.; Li, Q.; Hao, W.-F.; Cheng, J.-P. *J. Am. Chem. Soc.* **2002**, *124*, 9887.

SCHEME 2

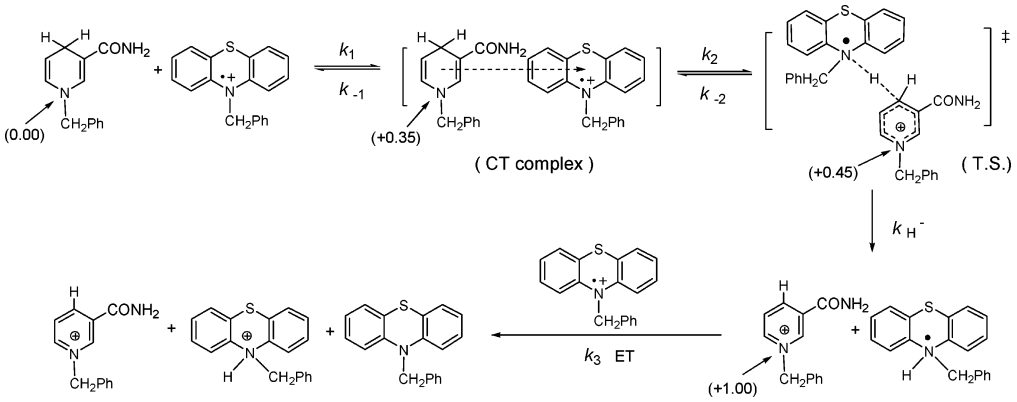

TABLE 6. Comparison of the Related Thermodynamic Data for the Various Reaction Systems with the Negative Kinetic Temperature Effect[a]

reaction system[b]	reaction type [c]	$\Delta H^{\ddagger}_{obs}$ [d]	$\Delta S^{\ddagger}_{obs}$ [e]	ΔH°_{inter} [d]	ΔS°_{inter} [e]	$\Delta H^{\ddagger}_{inter}$ [d]	$\Delta S^{\ddagger}_{inter}$ [e]	ref
TM-3	RR	−7.8	−44.7					21a
$AcrH_2$/DDQ	ET	−7.7	−40.7					28
$*Ru(bpy)_3^{2+}$/methyl *m*-nitrobenzoate	ET	−4.2	−42.3					20a
MH_2/DDQ	ET	−3.5	−44.2	−7.0	−10.3	3.5	−34.2	26
MH_2/DDQ	ET	−3.3	−	−8.8	−	5.7[f]		27
MGH/DDQ	ET	−3.2	−44.2	−11.0	−26.6	7.9	−17.7	26
BNAH/$PTZ^{\bullet+}$	H⁻T	−3.1	−34.9	−6.2	−4.6	3.1	−30.3	tw[g]
MAQ/$*Ru(bpy)_3^{2+}$	ET	−3.1	−32					17
$Fe^{II}(D_2bip)/Fe^{III}(Dbip)$	DT	−2.7	−50					15a
$Fe^{II}(H_2bip)$/TEMPO	HT	−2.7	−57	−9.4	−30	6.7[h]	−27[i]	15b
$*Ru(bpy)_3^{2+}$/*p*-nitrobenzaldehyde	ET	−2.6	−26.2					20a
MHOMe/DDQ	ET	−2.4	−43.3	−11.4	−28.2	9.0	−15.1	26
2,6-$(MeO)_2$Pyridine/$[(DH)_2Co(Me)(Py)]^+$	ET	−2.3	−52	<-6.9[j]				18
PhCCl/TME	AD	−2.3	−28					23a
$Fe^{II}(H_2bip)/Fe^{III}(Hbip)$	HT	−1.5	−45					15a
$Fe(H_2O)_6^{2+}/Ru(phen)_3^{3+}$	ET	−1.35	−36					13
DMA/TCNE	DA	−1.19	−41					12
$Fe(H_2O)_6^{2+}/Fe(terpy)_2^{3+}$	ET	−0.6	−38					13
ZnT(*t*-Bu)PP/$ZnT(t\text{-Bu})PP^{\bullet+}$	ET	−0.24	−4					16

[a] To facilitate the comparison, all units are converted to kcal·mol^{-1} or cal K^{-1} mol^{-1}. [b] Abbreviations: TM-3 = 3,5,5-trimethyl-2-oxomorpholin-3-yl radical; $AcrH_2$ = 10-methyl-9,10-dihydroacridine; DDQ = 2,3-dichloro-5,6-dicyano-*p*-benzoquinone; $*Ru(bpy)_3^{2+}$ = excited tris(2,2′-bipyridine)ruthenium(II); MH_2 = bis[4-(dimethylamino)phenyl]methane; MGH = Leuco Malachite Green; BNAH = benzyl-1,4-dihydronicotinamide; $PTZ^{\bullet+}$ = *N*-benzylphenothiazine radical cation; MAQ = 2-methylanthraquinone; $Fe^{II}(H_2bip)$ = iron 2,2′-bi(tetrahydro)pyrimidine; $Fe^{II}(D_2bip)$ = deuterated iron 2,2′-bi(tetrahydro)pyrimidine; Fe^{III}(Hbip) = iron bi(tetrahydro)pyrimidine; Fe^{III}(Dbip) = deuterated iron bi(tetrahydro)pyrimidine; TEMPO = 2,2,6,6-tetramethylpiperidine-*N*-nitroxyl radical; MHOMe = bis[4-(dimethylamino)phenyl]methoxymethane; DH = dimethylglyoxime; Py = pyridine; PhCCl = phenylchlorocarbene; TME = tetramethylethylene; $Ru(phen)_3^{3+}$ = tris(1,10-phenanthroline)ruthenium(III); DMA = 9,10-dimethylanthracene; TCNE = tetracyanoethylene. [c] RR = radical combination; ET = electron transfer; DT = deuterium-atom transfer; H⁻T = hydride transfer; HT = hydrogen-atom transfer; AD = carbine/alkene addition; DA = Diels−Alder reaction. [d] Units of kcal·mol^{-1}. [e] Units of cal K^{-1} mol^{-1}. [f] The original data take the value of 24 kJ·mol^{-1}. [g] This work. [h] Calculated with eq 3. [i] Calculated with the equation $\Delta S^{\ddagger}_{obs} = \Delta S^{\circ}_{CT} + \Delta S^{\ddagger}_{CT}$. [j] The value is estimated by the author. See ref 18.

state of the hydride transfer with negative temperature effect have been estimated. It is believed that this information would be valuable to understand the nature of the hydride transfer from NADH to the drug phenothiazine in vivo.

To search for the common origin resulting in the negative kinetic temperature effect on the reaction rate, the present reaction system and some reaction systems with negative kinetic temperature effect reported previously were summarized together in Table 6 for comparison. From Table 6, it is clear that most of the negative kinetic temperature effects were found to occur in the electron-transfer processes.[13,14,16−18,20,26−28] Although in some formal non-electron-transfer reactions, such as hydrogen atom transfer, hydride transfer, Diels−Alder reaction,[12] and carbine/alkene addition,[23a] the negative kinetic temperature effects can also be observed, in fact, these reactions are generally believed to be initiated by electron transfer or by concerted electron transfer, and it is reasonable to suggest that the electron transfer reaction should be the most common reaction type, which can result in negative kinetic temperature effect. The reason is that in the electron transfer process, the charge-transfer complex as reaction intermediate is easily formed, and the formation heat of the charge-transfer complex is frequently larger than the activation heat of the charge-transfer complex for the following reaction. From Table 6, we also find that the formation enthalpy (ΔH°_{inter}) of the charge-transfer complex generally is not too negative (generally larger than −12 kcal/mol). It is conceived that if the negative temperature effect can be observed on a reaction, the activation enthalpy of the intermediates ($\Delta H^{\ddagger}_{inter}$) should be quite small (generally smaller than 12 kcal/mol), which means that it is impossible to observe this unusual negative kinetic temperature effect in a very slow reaction. In fact, up until now, no paper has been released to report the negative kinetic temperature effect in a slow chemical reaction. As is well-known, electron transfer is universal in living bodies and the transfer rate generally is very fast, and it is reasonable to deduce that the reactions with negative kinetic temperature effects in vivo could not be few.

Conclusions

According to the examination of the kinetics, thermodynamics, and the reaction intermediate for the reaction of NADH analogue G-BNAH with the radical cation of *N*-benzylphenothiazine ($PTZ^{\bullet+}$) in acetonitrile, the following conclusions can be drawn:

(1) The rate of hydride transfer from G-BNAH to $PTZ^{\bullet+}$ decreased as the reaction temperature increased. The activation enthalpies of the hydride transfer all are negative values (−3.4 to −2.9 kcal/mol). The reason is that G-BNAH and $PTZ^{\bullet+}$ formed a charge-transfer complex prior to the hydride transfer from G-BNAH to $PTZ^{\bullet+}$ and the absolute value of the formation enthalpy for the CT-complex is larger than the activation enthalpy of the CT-complex, which results in negative values of the activation enthalpies for the hydride transfer from G-BNAH to $PTZ^{\bullet+}$.

(2) The reaction of G-BNAH with *N*-benzylphenothiazine radical cation ($PTZ^{\bullet+}$) in acetonitrile was initiated by the concerned hydride transfer via CT complex, rather than one-electron transfer, even though $PTZ^{\bullet+}$ was generally regarded as a typical one-electron oxidant.

(3) The effective charge distribution on the pyridine ring in G-BNAH at the stages of the CT-complex and the transition state was estimated to be 0.35 and 0.45 by using the method of Hammett-type linear free energy analysis.

(4) Since the structure of G-BNAH is quite close to the redox active center of NADH, it is reasonable to suggest that negative temperature effect could occur on the reactions of NADH coenzyme with the drug phenothiazine in vivo.

To our best knowledge, this paper not only reports the negative kinetic temperature effect on the reactions mediated by the NADH close analogue G-BNAH for the first time, but also provides detailed thermodynamic data (such as, state energy change) for each elementary step of the hydride transfer from the NADH analogue G-BNAH to $PTZ^{\bullet+}$ and the detailed charge distribution on G-BNAH at the various stages during the hydride transfer process, especially at the stage of CT-complex, and also examines the common origin resulting in the negative kinetic temperature effect on the chemical reactions, which, in fact, is never found in previous reports on this subject. It is evident that all this hard-to-get and very important information would be very valuable in understanding the nature of negative kinetic temperature effect, especially on the reactions mediated by NADH coenzyme in vivo.

Experimental Section

Materials. G-BNAH (G = *p*-OCH_3, *p*-CH_3, H, *p*-Cl, *p*-Br) and $PTZ^{\bullet+}ClO_4^-$ were synthesized according to the literature methods.[32,33] Reagent grade acetonitrile was refluxed over $KMnO_4$ and K_2CO_3 for several hours and was distilled over P_2O_5 under argon before use.

Kinetic and Spectral Measurement. The kinetic measurement of the reactions was carried out on an Applied Photophysics SX.18MV-R stopped-flow spectrometer, which was thermostated (±0.1 °C) by circulating water, by mixing the same concentration (1.0×10^{-4} M) of the two reactants. The SX.18MV-R uses a novel cell cartridge system that has a dead time of around 1 ms with very high sensitivity. The 5 μL cell with 1 mm path length light guide with a dead-time around 500 μs was applied in the experiments. The G-BNAH and $PTZ^{\bullet+}$ were weighed accurately by using an analytic balance (d = 0.01 mg) to ensure the some concentration of the two reactants. The spectra changes of $PTZ^{\bullet+}$ (λ_{max} = 512 nm, $\epsilon = 6.0 \times 10^3$ M^{-1} cm^{-1}) were monitored and the kinetic traces were recorded on an Acorn computer and analyzed by Pro-K Global analysis/simulation software, or translated to PC for further analysis. The well data fitting used the equation Abs = P1/(P1∗*k*∗*t* +1) + P2, which integrated in the Pro-K Global analysis/simulation software or Origin Software. The plot of 1/Abs vs time *t* would also give the same value of the rate constants. The corresponding observed rate constants was obtained by using the equation $k_{obs} = k \times \epsilon b$. In each case, it was confirmed that the rate constants derived from five to seven independent measurements agreed within an experimental error of ±5%. The equilibrium constant (K_{CT}) of the CT-complex was estimated from the initial absorbance of the CT-complex by changing the concentrations of G-BNAH according to the Benesi−Hildebrand equation (eq 2).[36] The corresponding thermodynamic parameters for the CT-complex formation were obtained from the plots of ln K_{CT} vs 1/T according to the van't Hoff equation (Supporting Information). The spectra of the CT complex were obtained by plotting the initial absorbance against the wavelength with the stopped-flow spectrophotometer. Other UV−vis spectra were performed on a HITACHI UV-3000 spectrometer.

Titrated Calibration Experiments. Titrated calibration experiments were performed in acetonitrile solution at 298 K on a CSC 4200 isothermal titration calorimeter. Prior to use, the instrument was calibrated against an internal heat pulse. Data points were collected every 2 s. The reaction heat of G-BNAH with $PTZ^{\bullet+}ClO_4^-$ was determined following nine automatic injections from a 250 μL injection syringe containing 2 mM G-BNAH into the reaction cell (1.00 mL) (containing 5 mM $PTZ^{\bullet+}ClO_4^-$). Injection volumes (10 μL) were delivered at 0.5 s intervals with 500 s between every two injections. The reaction heat was obtained by area integration of each peak except the first one.

Measurement of Redox Potentials. The electrochemical experiments were carried out by cyclic voltammetry (CV), Osteryoung square wave voltammetry (OSWV), and second-harmonic ac voltammetry (SHACV), using a BAS-100B electrochemical apparatus in deaerated acetonitrile solution under an argon atmosphere at 298 K as described previously.[9,40,46] *n*-Bu_4NPF_6 (0.1 M) was employed as the supporting electrolyte. A standard three-electrode cell consists of a glassy carbon disk as working electrode, a platinum wire as counter electrode, and 0.1 M $AgNO_3$/Ag (in 0.1 M Bu_4NPF_6−CH_3CN) as reference electrode. All sample solutions were about 1.5 mM. The ferrocenium/ferrocene redox couple ($Fc^{+/0}$) was taken as the internal standard.

Acknowledgment. Financial support from the Ministry of Science and Technology of China (Grant No. 2004CB719905), the National Natural Science Foundation of China (Grant Nos. 20125206, 20272027, 20332020, 20472038, and 20421202), Ministry of Education of China (Grant No. 20020055004), and Natural Science Fund of Tianjin (Grant No. 033804311) is gratefully acknowledged.

Supporting Information Available: Experimental details, thermodynamic cycles for calculating the change of the standard state enthalpy or free energy shown in Scheme 1, the electrochemical graphs for BNAH with three different electrochemical methods, and characterization spectra of BNAH and $PTZ^{\bullet+}$. This material is available free of charge via the Internet at http://pubs.acs.org.

JO061145C

(46) Arnett, E. M.; Venimadhavan, S. *J. Am. Chem. Soc.* **1991**, *113*, 6967.